31st Congress of the International Council
of the Aeronautical Sciences

Belo Horizonte, Brazil; September 09-14, 2018

PLY THICKNESS INFLUENCE IN COMPRESSION AFTER IMPACT DAMAGE ON CARBON/EPOXY TEST SPECIMENS

Thiago H. L. Pinto*, Carlos A. Cimini Jr, Sung K. Ha*****

***Universidade Federal dos Vales do Jequitinhonha e Mucuri, UFVJM, Rodovia MGT 367, km 583, 5000, Alto da Jacuba, Diamantina, 39100-000, MG, Brazil ,**

****Universidade Federal de Minas Gerais, UFMG, Av. AntÃť'nio Carlos 6627, Belo Horizonte, 31270-901, MG, Brazil ,**

*****Hanyang University, 222 Wangsimni-ro, Sageun-dong, Seongdong-gu, Seoul, South Korea**

Keywords: *Composite plates, Compression after impact (CAI), Finite elements, Ply thickness, Cohesive Elements*

Abstract

This study aims to map the ply arrangement and thickness influence on the impact damage, and subsequent compression damage, in composite compression after impact (CAI) test specimens, using Hashin failure criterion [20] as the main failure criteria. Both thick and thin ply models have standard CAI test specimen dimensions, with same thickness and different ply number. Also, different ply arrangements, as Quasi-isotropic and Cross-ply layups were considered. The specimens were modeled using 3D finite elements with and/or without inter-ply surfaces connected using cohesive elements [6]. Both thick and thin ply models have standard CAI test specimen dimensions [5], with same thickness and different ply number. Thick-to-thin ply thickness ratio was assumed to be 4. Quasi-isotropic and cross-ply layups were considered, with eight plies for the thick ply model, respectively stacked as $[+45/0/45/90]_S$ *and* $[0/90]_{2S}$*, and thirty-two plies for the thin ply model, respectively stacked as* $[+45/0/45/90]_{4S}$ *and* $[0/90]_{8S}$*.*

Complex test programs are still necessary to fully characterize the material and the failure modes in order to develop accurate numerical methods, however, based in this study is possible to evaluate the effects of damage generated due to compression after low velocity impact in carbon/epoxy composite laminates. The goal of this work is to fully understand the possible benefits offered by different ply thickness in composite materials, being possible to observe, based on preliminary studies, a tendency of greater local stiffness and residual strength for thin laminates.

1 Introduction

Composite materials are ideal for structural applications where high strength-to-weight and stiffness-to-weight ratios are required. Since the antiquity, humanity uses different materials combinations in order to improve products quality. From the early days, it's observed the use of wood, a natural composite material considering the fact that its properties vary significantly with and against the fiber directions. Over time, materials have been specialy developed in order to build goods: from houses and facilities built from primitive mud bricks reinforced with straw, later replaced by steel bars reinforced concrete, to the modern airframe structures built from fiber reinforced composites [30]. Composites are widely used in the manufacture of a variety of products, ranging from aircrafts, spacecrafts, missiles and rockets, to sport goods, marine and automobile components, and biomedical aplications [11, 38].

The impact damage generated in composite laminates has been a recurring theme of interest to researchers since it leads to Compression After impact (CAI) phenomena, the most critical design tolerance in aerospace structures, and has to be analyzed using expensive and time-consuming experiments. Experimental and simulation results have been widely analyzed and published, including review articles on the current state of the art, studying issues such as new analytical methods to represent test results [39, 8], the variation of constitutive properties in impact resistance in continuous fibers reinforced composite materials to improve impact properties [7, 23, 19, 28, 32, 26], determination of the strain fields and failure mechanisms during the failure of the impacted composite laminates when subjected to compression [24, 27, 40], the impact induced crack propagation [36], and the analysis of these effects in delamination prediction methods [14, 18], as the contact radius increase due to deflection, delamination, and damage evolution in low velocity impact [45, 25, 3, 41, 42, 35, 15]. Different perspectives, with respective computational cost particularities, can be chosen, as two-dimensional simulations [12, 10, 43] and three-dimensional [22]. Impact tests may be performed experimentally with different apparatus, as impact hammer or drop tower, as described by [9], [17], [31], [21], [37], and [44]. Special attention needs to be taken, during tests and/or numerical model development, in order deal with and incorporate nonlinear behaviors such as material degradation and large deformations in the results. The impact damage positions effect affects and is affected by the buckling and post-buckling behaviors of stiffened composite panels under axial compression [16, 2].

Most composite materials are reinforced with strong and stiff fibers, if compared with it's matrix portion, leading to a clear distinction between fiber and inter-fiber (matrix, interface) failure modes. Those characteristics allows a failure a simplified and more physically significant failure treatment in the case of maximum stress, maximum strain and fully interactive theories [11]. The Puck and Schurmann [34] modified three dimensional Hashin failure criteria is applied in order to model anisotropic damage in fiber-reinforced materials. The response of the undamaged material is assumed to be linearly elastic, and the model is intended to predict behaviour of fiber-reinforced materials for which damage can be initiated without a large amount of plastic deformation. The Hashin's initiation criteria are used to predict the onset of damage, and the damage evolution law is based on the energy dissipated during the damage process and linear material softening. Four different modes of failure are considered: fiber rupture in tension; fiber buckling and kinking in compression; matrix cracking under transverse tension and shearing; and matrix crushing under transverse compression and shearing [20].

2 Methodology

For a CAI problem, the influence of thick versus thin ply composite laminates was evaluated using the Puck and Schurmann [34] modified Hashin failure criterion. Both thick and thin ply models have standard CAI test specimen dimensions [5], with same thickness and different ply number. Quasi-isotropic and cross-ply layups were considered, with eight plies for the thick ply model, disposed as $[+45/0/45/90]_S$ and $[0/90]_{2S}$ respectively for each case, and thirty-two plies for the thin ply model, disposed as $[+45/0/45/90]_{4S}$ and $[0/90]_{8S}$ respectively for each case. In a second study, the cross-ply layups ($[0/90]_{2S}$ and $[0/90]_{8S}$ for thick and thin ply models, respectively) using the same modified Hashin failure criterion [34], where the Cohesive Failure Criteria [6] was inserted in order to verify the influence of the delamination model in these results.

2.1 Puck and Schurmann [34] modified three dimensional Hashin failure criteria

This failure criteria, implemented for Abaqus using a VUMAT named *uniFiber.f* [29] (available in Abaqus documentation [1]) is based on Hashin's failure criteria for unidirectional fiber composites [20], using the constitutive model with minor modifications for fibers. For the matrix failure modes, a constitutive model based on

Puck's action plane theory [34] was developed for both tension and compression cases. In this [34] modified three dimensional Hashin failure criteria, four distinct failure modes were considered: tensile fiber failure, compressive fiber failure, tensile matrix failure, and compressive matrix failure, expressed mathematically as below [29].

Fiber tension ($\sigma_{11} > 0$):

$$F_f^T = \left(\frac{\sigma_{11}}{X_T}\right)^2 + \left(\frac{\sigma_{12}}{S_{12}}\right)^2 + \left(\frac{\sigma_{13}}{S_{13}}\right)^2 \quad (1)$$

Fiber compression ($\sigma_{11} < 0$):

$$F_f^C = \left(\frac{\sigma_{11}}{X_C}\right) \quad (2)$$

Matrix tension ($\sigma_{22} + \sigma_{33} > 0$):

$$F_m^T = \left(\frac{\sigma_{11}}{2X_T}\right)^2 + \left(\frac{\sigma_{22}^2}{Y_T Y_C}\right) + \left(\frac{\sigma_{12}}{S_{12}}\right)^2 + \left(\frac{\sigma_{22}}{Y_T Y_C}\right) \quad (3)$$

Matrix compression ($\sigma_{22} + \sigma_{33} < 0$):

$$F_m^C = \left(\frac{\sigma_{11}}{2X_T}\right)^2 + \left(\frac{\sigma_{22}^2}{Y_T Y_C}\right) + \left(\frac{\sigma_{12}}{S_{12}}\right)^2 + \left(\frac{\sigma_{22}}{Y_T Y_C}\right) \quad (4)$$

where S_{12}, S_{13} and S_{23} denote allowable shear strengths in the respective principal material directions. One may observe that, besides being defined as a material input for this Abaqus documentation [1] available VUMAT (*uniFiber.f*), the transverse shear strength (S_{23}) is not used during the failure criteria.

2.2 Cohesive Failure Criteria

Complementarily to the aforementioned intra-laminar failure criteria, it is proposed the use an inter-laminar criteria, since delamination, as a result of impact, or even due to manufacturing defects, can cause a significant reduction in the compressive load-carrying capacity of a structure [6]. The cohesive damage initiation refers to the beginning of cohesive response degradation at a contact point, which begins when the contact stresses and/or contact separations satisfy the specified damage initiation criteria.

Using the *Quadratic stress criterion*, damage is assumed to initiate when a quadratic interaction function involving the contact stress ratios (as defined in the expression below) reaches a value of one. This criterion can be represented as [1]:

$$\left\{\frac{< t_n >}{t_n^o}\right\}^2 + \left\{\frac{t_s}{t_s^o}\right\}^2 + \left\{\frac{t_t}{t_t^o}\right\}^2 = 1 \quad (5)$$

Where $\mathbf{t}$ is the nominal traction stress vector in normal and first/second shear directions (n, s and t respectively). $\mathbf{t}^o$ denotes the nominal traction stress limit. The Macaulay brackets (<>) are used to signify that a purely compressive displacement (i.e., a contact penetration) or a purely compressive stress state does not initiate damage.

3 Analysis and Results

The studies presented herein aims to map the ply arrangement and thickness influence on the impact damage, in composite compression after impact (CAI) test specimens, using Hashin failure criterion [20] as the main failure criteria. Both thick and thin ply models have standard CAI test specimen dimensions, with same thickness and different number of plies. Also, different ply arrangements, as Quasi-isotropic and Cross-ply layups were considered. The specimens were modeled using 3D finite elements and both thick and thin ply models have standard CAI test specimen dimensions [5], with same thickness and different ply number. Thick-to-thin ply thickness ratio was assumed to be 4. Quasi-isotropic and cross-ply layups were considered, with eight plies for the thick ply model, respectively stacked as $[+45/0/-45/90]_S$ and $[0/90]_{2S}$, and thirty-two plies for the thin ply model, respectively stacked as $[+45/0/-45/90]_{4S}$ and $[0/90]_{8S}$. Figure 1 presents a cross section view of the aforementioned ply arrangements. The goal of this work is to fully understand the possible benefits offered by different ply thickness in composite materials, being possible to observe, based on preliminary studies, a tendency of greater local stiffness and residual strength for thin laminates.

For computational time reduction proposes, the model presented in the cross-ply results is a model with two symmetry planes, only a quarter of the plate is shown in the Figure 2 (right). The planes of symmetry are placed in top and left borders, the impact point being the upper left end, and the support constraints applied to the bottom and right. Due to the quasi-isotropic layups characteristics, the planes of symmetry, XZ and YZ, are not functional and, for quasi-isotropic analyses, the complete model (Figure 2 left) were used. Besides this simplification, the results are presented in complete domain, so mirroring the cross-ply results in both symmetry planes.

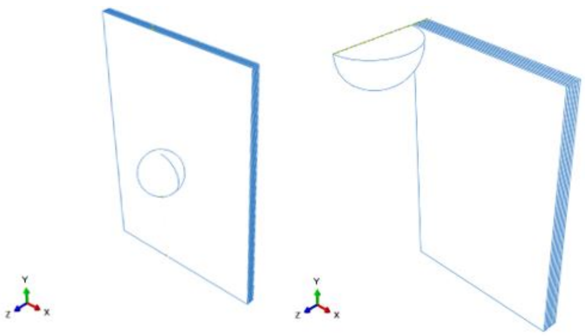

Fig. 2 : Representation of complete model (left) and simplified model where two planes of symmetry were applied (right).

A unidirectional carbon/epoxy material is defined to each lamina, using the elastic properties shown in Table 1 [11].

Table 1: Elastic properties of the unidirectional carbon/epoxy ply.

E_{11} $[MPa]$	E_{22} $[MPa]$	E_{33} $[MPa]$	ν_{12}	ν_{13}	ν_{23}	G_{12} $[MPa]$	G_{13} $[MPa]$	G_{23} $[MPa]$
164000	12000	12000	0.32	0.32	0.45	4500	4500	2500

The allowable strength values adopted in this work are presented in Table 2 [11].

Table 2: Allowable stresses of the unidirectional carbon/epoxy ply.

X_1^t $[MPa]$	X_1^c $[MPa]$	X_2^t $[MPa]$	X_2^c $[MPa]$	X_3^t $[MPa]$	X_3^c $[MPa]$
2724	1690	50	111	290	290

The shear strength of the unidirectional carbon/epoxy ply presented is shown in Table 3 [11].

Table 3: Shear strength of the unidirectional carbon/epoxy ply.

S_{12} $[MPa]$	S_{13} $[MPa]$	S_{23} $[MPa]$
120	137	90

For models with interface failure criteria, the cohesive layer properties are presented in Table 4 [13].

Table 4: Interface properties.

G_{1c} $[N/mm]$	G_{2c} $[N/mm]$	$\tau^{\circ}{}_3$ $[MPa]$	$\tau^{\circ}{}_{shear}$ $[MPa]$	η
0.969	1.719	80	100	2.28

Based on the results from previous work from the authors [33], summarized in Figure 3, it is possible foresee a reduction of expected damage as a reduction in ply thickness influence, due to sub-laminate scaling, besides this behavior corroborates with logical micro-structural effects expectation, such as lower probability of occurrence of micro-cracks, probability of critical defects, wich were not included in the presented model. The problem results may be described

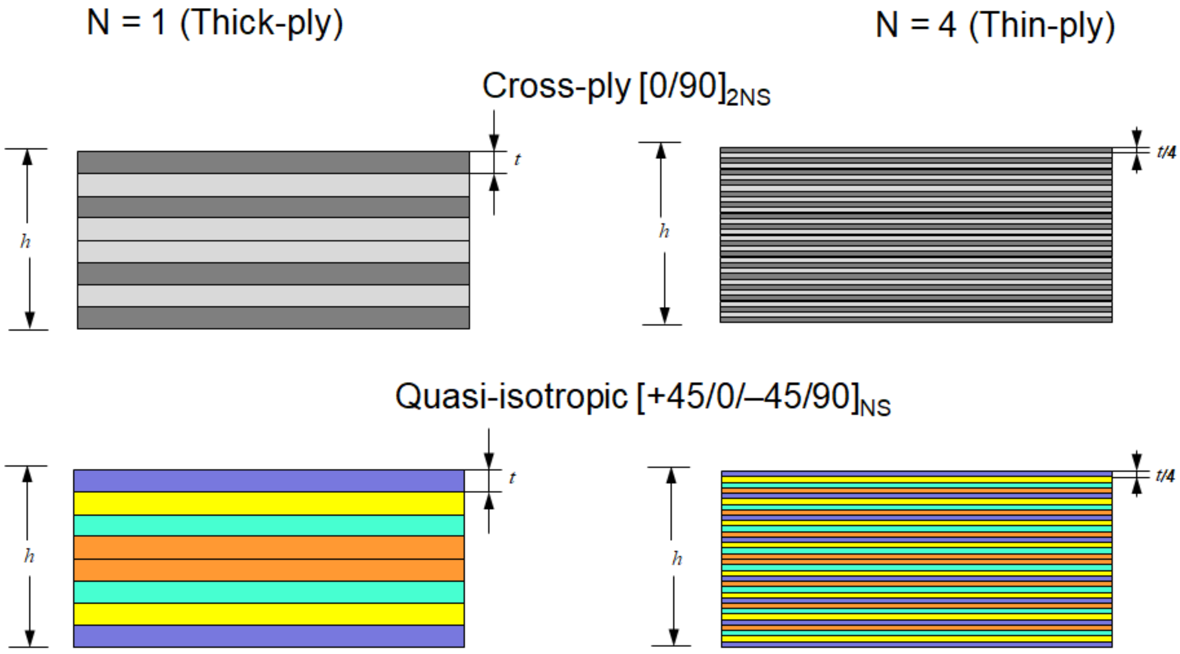

Fig. 1 : Cross section view of proposed ply arrangements.

as up-scaling in laminate thickness, wich can be achieved by either changing the number of identical plies in the laminate thickness, known as blocked laminate arrangement, or by repeating the lay-up sequence several times using a single ply for each orientation, known as sub-laminated arrangement. Each of these configurations leading to different results due to the triggering of different failure mechanisms [4].

3.1 Quasi-Isotropic Layups $[+45/0/45/90]_{NS}$

Due to the quasi-isotropic layups caracteristics, the planes of symmetry, XZ and YZ, were not applied for Quasi-Isotropic Layups models. Three-dimensional model meshes, with a total of 148,513 hexahedral elements, were developed. However, thick and thin ply meshes still differ in the number of nodes due to their different number of inter-ply connections: 186,838 nodes for the thick ply model and 298,390 nodes for the thin ply model. A 3J and a 17J energy impact of a rigid sphere, using iced water density in order to simulate a hail impact was replicated in both models. Figure 4 presents the ply thickness influence in CAI results, where the after compression final matrix damage states are shown for specimens with no previous impact, and subjected to 3J and 17J impacts.

The ply thickness influence in CAI Residual Strength results is shown in Figure 5, presenting the maximum compression force for each case above. One may observe a tendency of greater residual strength for thin laminates, which remains even after loss of rigidity due to impact.

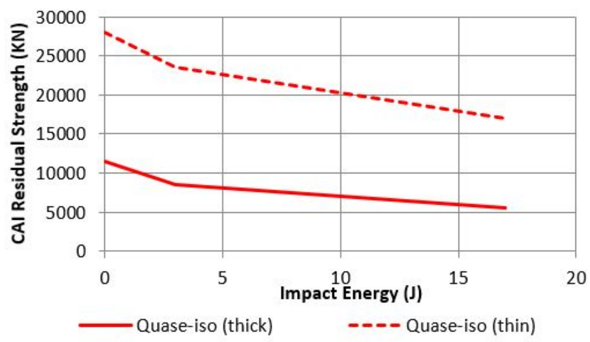

Fig. 5 : CAI Residual Strength for Quasi-Isotropic Layups ($[+45/0/45/90]_{NS}$).

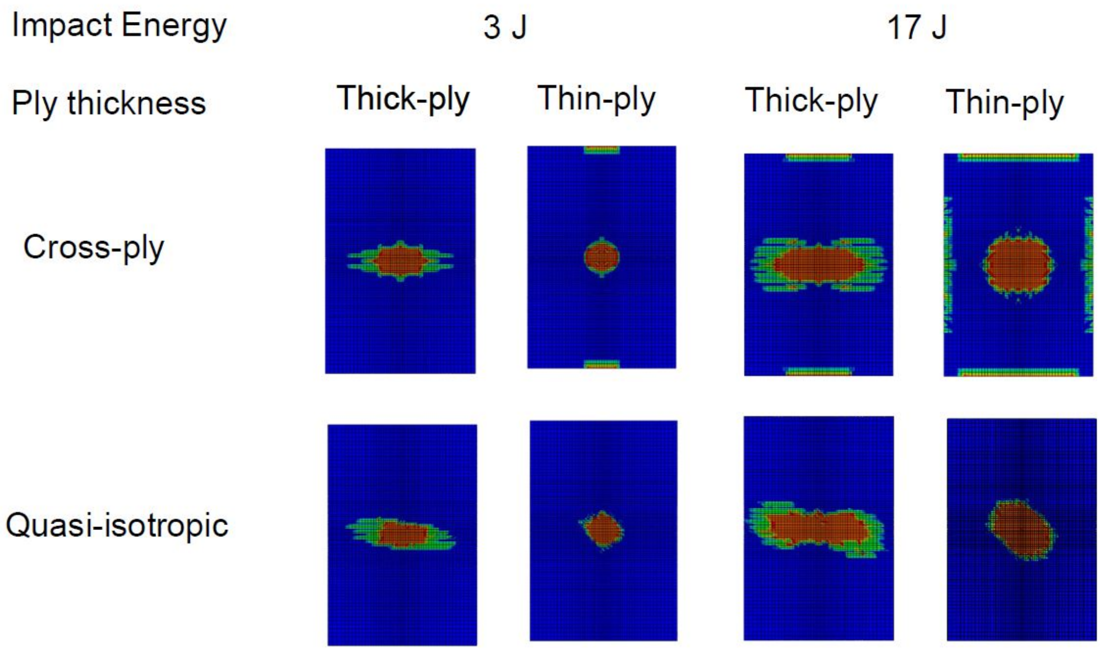

Fig. 3 : Summary of impact analysis [33].

3.2 Cross-Ply Layups $[0/90]_{2NS}$

Using the symmetry described above, three-dimensional model meshes with a total of 35,424 hexahedral elements were developed. However, thick and thin ply meshes differ in the number of nodes due to their different number of inter-ply connections: 47,364 nodes for the thick ply model and 75,588 nodes for the thin ply model. In order to reduce the computational time, two planes of symmetry, XZ and YZ, were applied. A 3J energy impact of a rigid sphere, using iced water density in order to simulate a hail impact was replicated in both models. Figure 6 presents the ply thickness influence in CAI results, where the after compression final matrix damage states are shown for specimens with no previous impact, and subjected to 3J and 17J impacts.

The same model were then modified, including the cohesive elements [6] inter-ply surfaces connection, in order to verify the influence of the delamination model in the results. Figure 7 (top) presents the ply thickness influence in CAI results, where the after compression final matrix damage states are shown for specimens with no previous impact, and subjected to 3J and 17J impacts. The bottom part of Figure 7 presents the last interface (opposite to impact) delamination states at the final damage states.

The ply thickness influence in CAI Residual Strength results is shown in Figure 8, presenting the maximum compression force for each case with and without the cohesive model. One may observe a tendency of greater residual strength for thin laminates, which remains even after loss of rigidity due to impact, present in both with and without cohesive model cases.

4 Conclusions

Analyzing the simulation results for the Compression After Impact damage generated in the laminate presented in this work, it's possible to observe a tendency of greater residual strength

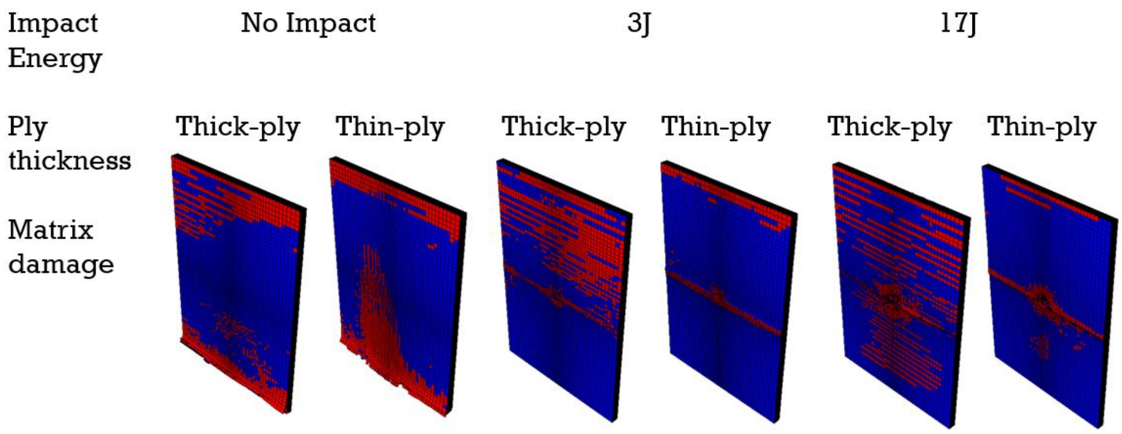

Fig. 4 : Summary of CAI analysis for Quasi-Isotropic Layups ($[+45/0/45/90]_{NS}$).

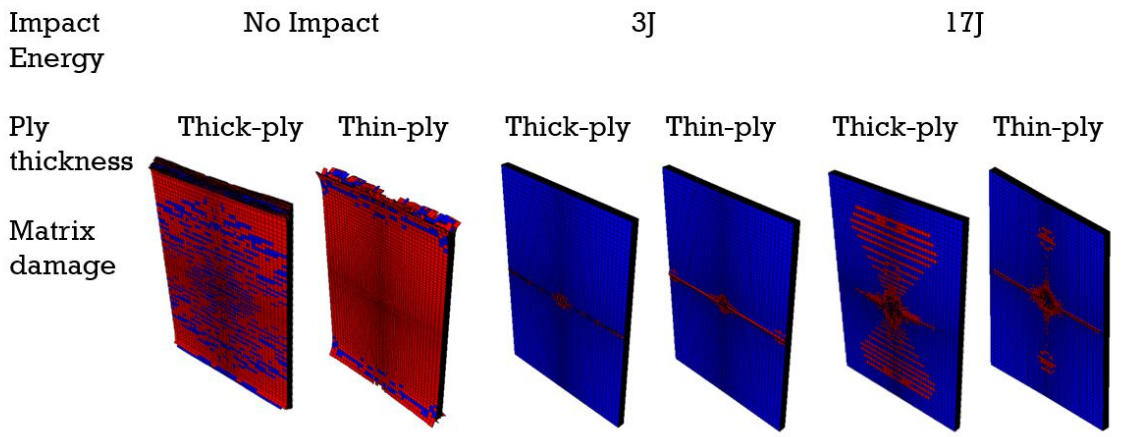

Fig. 6 : Summary of CAI analysis for Cross-Ply Layups ($[0/90]_{2NS}$).

for thin laminates, which remains even after loss of rigidity due to impact, present in both with and without cohesive model cases. Besides that impact damage, ad it's effect in after impact loads, can't be entirely avoided, it is useful to understand the mechanical behavior of the material and the modification of this behavior due to rearrangement of plies. Complex test programs are necessary to fully characterize the material and the failure modes in order to develop accurate numerical methods, however, based in this study is possible to evaluate the effects of damage generated due to low velocity impact in carbon/epoxy composite laminates, and the effect regarding to compression after impact (CAI) residual strength. Based on the above results it is possible foresee a increase in the compression after impact (CAI) residual strength due to the ply thickness reduction, so using more plies and the same amount of material, on the impact damage, and after impact load, in carbon/epoxy composite. This behavior corroborates with the expectation of lower probability of occurrence of microcracks. On the other hand, the use of thinner plies may increase the costs of manufacturing and, at some point, even be impossible to manufacture.

References

[1] ABAQUS, *CAE user's manual, version 6.14*. Dassault Systemes, 2014.

[2] Abir, M., Tay, T., Ridha, M. and Lee, H. *On the relationship between failure mechanism and compression after impact (CAI) strength in composites*. Composite Structures 182, 242-250, 2017.

[3] Abir, M., Tay, T., Ridha, M. and Lee, H. *Mod-*

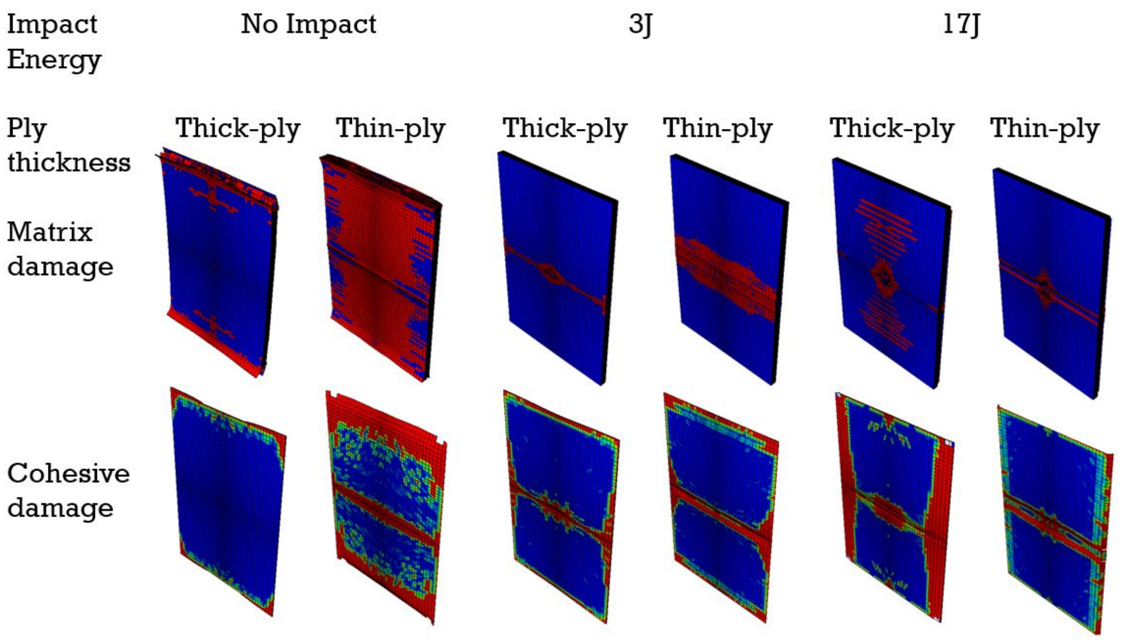

Fig. 7 : Summary of CAI analysis for Cross-Ply Layups ($[0/90]_{2NS}$) with Cohesive Failure Criteria.

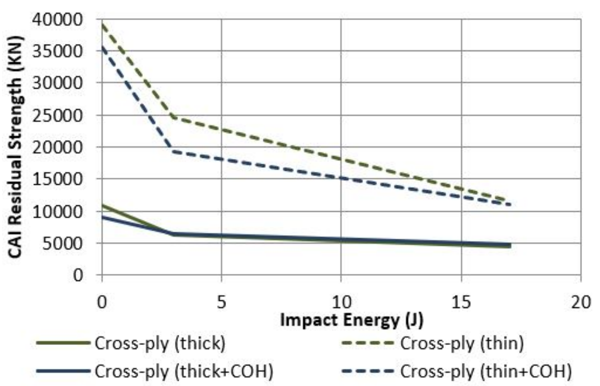

Fig. 8 : CAI Residual Strength for Cross-Ply Layups ($[0/90]_{2NS}$).

elling damage growth in composites subjected to impact and compression after impact. Composite Structures 168, 13-25, 2017.

[4] Amacher, R., Cugnoni, J., Botsis, J., Sorensen, L., Smith, W. and Dransfeld, C. *Thin ply composites: Experimental characterization and modeling of size-effects*. Composites Science and Technology 101, 121-132, 2014.

[5] ASTM D7137/D7137M-12, *Standard test method for compressive residual strength properties of damaged polymer matrix composite plates*. ASTM International, West Conshohocken, PA, USA, 2012.

[6] Camanho, P. P. and DÃąvila, C. G. *Mixed-mode decohesion finite elements for the simulation of delamination in composite materials*. NASA/TM-2002-211737, NASA CASI (Center for AeroSpace Information), Hanover, MD, USA, 2002.

[7] Cantwell, W. and Morton, J. *The impact resistance of composite materials - a review*. Composites 22(5), 347-362, 1991.

[8] Caprio, F. D., Langella, A., Lopresto, V. and Caprino, *Numerical, experimental and analytical correlation for predicting the structural behavior of composite structures under impact*. Procedia Engineering 167, 80-87, 2016.

[9] Choi, H. Y. and Chang, F.-K. *A model for predicting damage in graphite/epoxy laminated composites resulting from low-velocity point impact*. Journal of Composite Materials 26(14), 2134-2169, 1992.

[10] Christoforou, A. P. and Yigit, A. S. *Scaling of low-velocity impact response in composite structures*. Composite Structures 91(3), 358-365, 2009.

[11] Daniel, I. and Ishai, O. *Engineering Mechanics of Composite Materials - 2nd ed.* OXFORD UNIV PR., 2005.

[12] Davies, G. and Zhang, X. *Impact damage prediction in carbon composite structures*. International Journal of Impact Engineering 16(1),

149-170, 1995.

[13] Davila, C. G., Camanho, P. P. and Turon, A. *Cohesive elements for shells*. Technical Report TP-2007-214869, NASA, 2007.

[14] Elder, D. J., Thomson, R. S., Nguyen, M. Q. and Scott, M. L. *Review of delamination predictive methods for low speed impact of composite laminates*. Composite Structures 66(1-4), 677-683, 2004.

[15] Feng, D. and Aymerich, F. *Finite element modelling of damage induced by low-velocity impact on composite laminates*. Composite Structures 108, 161-171, 2014.

[16] Feng, Y., Zhang, H., Tan, X., He, Y., An, T. and Zheng, J. *Effect of impact damage positions on the buckling and post-buckling behaviors of stiffened composite panel.* Composite Structures 155, 184-196, 2016.

[17] Gonzales, M. A. C., Dias, R. P. and Alves, M. *An experimental-numerical analysis of the drop weight tear test*. 20th International Congress of Mechanical Engineering, 2009.

[18] Gonzalez, E., Maimi, P., Camanho, P., Turon, A. and Mayugo, J. *Simulation of drop-weight impact and compression after impact tests on composite laminates*. Composite Structures 94(11), 3364-3378, 2012.

[19] Han, G., Guan, Z., Li, X. and Du, S. *Failure analysis of carbon fiber reinforced composite subjected to low velocity impact and compression after impact*.Journal of Reinforced Plastics and Composites 35(9), 727-746, 2016.

[20] Hashin, Z. *Failure Criteria for Unidirectional Fiber Composites*. Journal of Applied Mechanics, 47, pp. 329-334, 1980.

[21] Hazzard, M. K., Hallett, S., Curtis, P. T., Iannucci, L. and Trask, R. S. *Effect of fibre orientation on the low velocity impact response of thin dyneema composite laminates*. International Journal of Impact Engineering 100, 35-45, 2017.

[22] Hou, J., Petrinic, N., Ruiz, C. and Hallett, S. *Prediction of impact damage in composite plates*. Composites Science and Technology 60(2), 273-281, 2000.

[23] Justo, J., Osuna, S. and Paris, F. *Design of composite materials with improved impact properties*. Composites Part B: Engineering 76, 229-234, 2015.

[24] Kadlec, M. and Kafka, V. *Strain concentration during the compressionof a carbon/epoxy composite after impact*. International Journal of Structural Integrity 6(2), 279-289, 2015.

[25] Li, N. and Chen, P. *Micro-macro FE modeling of damage evolution in laminated composite plates subjected to low velocity impact*. Composite Structures 147, 111-121, 2016.

[26] Liu, H., Falzon, B. G. and Tan, W. *Predicting the compression-after-impact (CAI) strength of damage-tolerant hybrid unidirectional/woven carbon-fiber reinforced composite laminates*. Composites Part A: Applied Science and Manufacturing 105, 189-202, 2018.

[27] Liu, P., Liao, B., Jia, L. and Peng, X. *Finite element analysis of dynamic progressive failure of carbon fi
ber composite laminates under low velocity impact*. Composite Structures 149, 408-422, 2016.

[28] Liv, Y., Guillamet, G., Costa, J., GonzÃąlez, E., Marin, L. and Mayugo, J. *Experimental study into compression after impact strength of laminates with conventional and nonconventional ply orientations*. Composites Part B: Engineering 126, 133-142, 2017.

[29] Nie, Z. *Advanced mesomechanical modeling of triaxially braided composites for dynamic impact analysis with failure*. Master's thesis, University of Akron, 2014.

[30] Niu, M. C. Y. *Composite Airframe Structures*. Hong Kong Conmilit Press Ltd., 2010.

[31] Olsson, R. *Analytical model for delamination growth during small mass impact on plates*. International Journal of Solids and Structures 47(21), 2884-2892, 2010.

[32] Perillo, G., Jorgensen, J. K., Cristiano, R. and Riccio, A. *A numerical/experimental study on the impact and CAI behaviour of glass reinforced compsite plates*. Applied Composite Materials 25(2), 425-447, 2017.

[33] Pinto, T. H. L., Cimini Jr., C. A., Ha, S. K., Cabral, P. H., Silva, G. H. C. and Prado, A. P. *Ply thickness in uence in impact damage on cai carbon/epoxy test specimens*. 21st International Conference on Composite Materials, Xi'an, 20-25th August 2017'.

[34] Puck, A. and Schurmann, H. *Failure analysis*

of FRP laminates by means of physically based phenomenological models. Composites Science and Technology 58, 1045-1067, 1998.

[35] Richardson, M. and Wisheart, M. *Review of low-velocity impact properties of composite materials*. Composites Part A: Applied Science and Manufacturing 27(12), 1123-1131, 1996.

[36] Rivallant, S., Bouvet, C., Abdallah, E. A., Broll, B. and Barrau, J.-J. *Experimental analysis of CFRP laminates subjected to compression after impact: The role of impact-induced cracks in failure*. Composite Structures 111, 147-157, 2014.

[37] Santiago, R., Cantwell, W. and Alves, M. *Impact on thermoplastic fibre-metal laminates: Experimental observations*. Composite Structures 159, 800-817, 2017.

[38] Srinivasan, K. *Composite Materials: Production, Properties, Testing and Applications*. Alpha Science Intl Ltd, 2009.

[39] Suemasu, H. *Analytical approaches to compression after impact (CAI) behavior of carbon fiber-reinforced composite materials*. Advanced Composite Materials 25(1), 1-18, 2016.

[40] Sun, X. and Hallett, S. *Failure mechanisms and damage evolution of laminated composites under compression after impact (CAI): Experimental and numerical study*. Composites Part A: Applied Science and Manufacturing 104, 41-59, 2018.

[41] Tan, W., Falzon, B. G., Chiu, L. N. and Price, M. *Predicting low velocity impact damage and compression-after-impact (CAI) behaviour of composite laminates*. Composites Part A: Applied Science and Manufacturing 71, 212-226, 2015.

[42] Tan, W., Falzon, B. G., Chiu, L. N. S. and Price, M. *Numerical prediction of the low-velocity impact damage and compression after impact strength of composite laminates*. IOP Conference Series: Materials Science and Engineering 74, 12-15, 2015.

[43] Tiberkak, R., Bachene, M., Rechak, S. and Necib, B. *Damage prediction in composite plates subjected to low velocity impact*. Composite Structures 83(1), 73-82, 2008.

[44] Yasaee, M., Mohamed, G., Pellegrino, A., Petrinic, N. and Hallett, S. R. *Strain rate dependence of mode II delamination resistance in through thickness reinforced laminated composites*. International Journal of Impact Engineering 107, 1-11, 2017.

[45] Yu, Z. and Gao, S. *Increase of contact radius due to de ection in low velocity impact of composite laminates and prediction of delamination threshold load*. Composite Structures 147, 286-293, 2016.

5 Acknowledgments

The first author is a CAPES scholar from Doctoral Sandwich Abroad Program (in portuguese: Programa de Doutorado Sanduíche no Exterior - PDSE), edital no. 47/2017, process number 88881.187859/2018-01.

The authors are thankful for the assistance of the Structural Engineering Department of UFMG, the Department of Mechanical Engineering of Hanyang University, and Embraer S.A. This work was supported by CAPES, CNPq, and FAPEMIG.

6 Contact Author Email Address

For correspondence, please contact: thiago.lara@ict.ufvjm.edu.br .

Copyright Statement